Zagazig University Medical Journal
www.zumj.journals.ekb.eg
https://doi.org/10.21608/zumj.2024.234154.2873 Volume 30, Issue 4, July 2024
Manuscript ID ZUMJ-2311-3012 (R2)
DOI 10.21608/ZUMJ.2023.250804.3012

Original Article

Role of Multislice Computed Tomography Angiography in Association with Virtual Computed Tomography in Diagnosis of Aortic Dissection

Amira Abd EL-Mageed Mohsenah[1*], Mohammed Ahmed Denewar[1], Samar Mohamad Shehata[1], Dalia Salah El Deen Anwar[1]

[1]Radiodiagnosis Department, Faculty of Medicine, Zagazig university,Egypt

***Corresponding author:**
Amira Abd EL-Mageed Mohsenah
Email:
amiramohsna@gmail.com

Submit Date 2023-11-23
Revise Date 2023-12-25
Accept Date 2023-12-28

ABSTRACT

Background: Aortic dissection (AD) is a highly fatal disease, especially type A; the mortality rate increases with late diagnosis of dissection, and lots of cases die before diagnosis or once diagnosed due to massive complications. However, it is male-predominant, and more complications affect females. This study aimed to assess the role of Multidetector Computed Tomography (MDCT) in the diagnosis of aortic dissection and the added value of virtual CT.

Methods: This retrospective study was conducted at the Radiodiagnosis Department at Zagazig University Hospitals and Radiodiagnosis Department, national cardiac institute. The study included 18 patients who proved on examination by CT to have aortic dissection, double aortic lumen, and the presence of a dissecting flap. There were 14 males (77.7%) and four females (22.3%). Their ages ranged from 32 to 86 years (mean age: 60.39 ±13.980 years).

Results: Virtual CT provides a unique picture of the aorta from the inside and provides a more accurate characterization of the tears and flaps. Nine cases had irregular entry tears, and six cases had rounded ET, sheet-like in 10 cases, and wave-like in four cases. The intimal tear display quality was fair in three cases, satisfactory in five cases, and optimal in 10 cases.

Conclusions: Because of its efficiency, accessibility, and sensitivity, MDCTA is the preferred approach for diagnosing individuals with suspected AD. It enables a thorough evaluation of the aorta and its branches; even the involvement of the small aortic branches, such as coronary arteries, can be proved by virtual CT angioscopy.

Keywords: Aortic dissection, MDCTA, virtual CT, CT Angiography

INTRODUCTION

Aortic dissection is a potentially fatal cardiovascular condition that occurs when the aortic intima tears and blood leaks into the media. Aortic intramural hematoma in a few people may also lead to subsequent dissection [1]. The false lumen rapidly expands down the longitudinal axis of the aorta as a result of the continuous inflow of blood, potentially leading to an aortic wall rupture [2].

The prevalence of Aortic dissection in the overall population is roughly 6/100,000 per year, and it is likely to rise with age. In the first International Registry of Acute AD (IRAD) release, the overall mortality of AD was 27.7%; the early death of AD cases

without suitable therapy was 1% - 2% per hour [3].

The most frequently utilized imaging modality for the identification and management of AD is computed tomography angiography (CTA), with a sensitivity and specificity of about 100%, particularly for individuals who intend to receive endovascular therapy [4].

MDCTA can be used to assess the intimal tear's original site and extent, as well as the size of the false lumen and involvement of the branch vessels, all of which are relevant to the patient's care and prognosis [5]. This study aimed to estimate the role of MDCT in the evaluation of AD and the added value of virtual CT angioscopy.

METHODS

This retrospective study was performed at the Radiodiagnosis Department at Zagazig University Hospitals and the Radiodiagnosis Department at the National Cardiac Institute. The study included 18 patients who proved on examination by CT to have aortic dissection. All cases proved by MDCT in the form of the presence of a dissection flap (DF) and the presence of double aortic lumens. There were 14 males and four females. Their ages ranged from 32 to 86 years, and their mean age was 60.39 ±13.980 years. The research was conducted under the World Medical Association's Code of Ethics (Helsinki Declaration) for human research. This study was carried out after the approval of the Institutional Review Board (IRB) (#5906).

All cases with suspected acute aortic syndrome proved to be AD on MDCT examination were included in the current study.

Cases with the following characteristics were excluded: pregnant females, impaired renal function, allergy to contrast media, and hemodynamic instability.

A detailed history was taken from the patients (Age, history of any present complaints, allergic reaction to contrast agent, HPT, trauma, or previous operations). Routine laboratory investigation, including renal function test, revising previous investigations (radiological, laboratory), and radiological examination.

128-slice MDCTA scanner (ingenuity Philips health care, best, Netherlands) was used for nine patients, 64 MDCTA (Siemens Medical Systems) was used for five patients, and (Canon Medical System) MDCT was used for four patients; all studies were transferred to a Paxera ultima and a dedicated Philips work station for Post-processing of images including multiplanar reconstruction (MPR), maximum intensity projections (MIPs), volume rendering (VR), curved reconstruction (C-MPR), and Virtual angioscopy.

Patients were positioned in a comfortable supine position with their arms up, respiratory training to hold their breath for 10 seconds. An I.V. cannula was inserted in the antecubital vein. A 120 ml Iohexol with an iodine concentration of 350 mg was injected intravenously at a flow rate of 5.5 ml/s, and anti-allergic measures were taken. The start time of imaging was settled in each patient by computer-assisted bolus tracking. ECG leads were positioned for ECG gating. The scout was acquired with the patient in a supine position with head first. The axial cuts were taken from the base of the neck to the symphysis pupils; the scan area extended from the root of the neck to the bifurcation of the aorta.

***CT imaging technique*:** ECG-gated MDCT angiography was performed. The following parameters were used to generate the MDCT protocol: 40 cm field of view, 0.3 pitch, standard abdominal filter, 0.6 mm for both collimation width and reconstruction

increment, X-ray tube rotation time (0.4 s), tube current (400–700 mAs), and tube voltage (80–100 kV). The median and mean thickness of chest slices, respectively, were 1.25 mm and 1.94 mm. The thickness of an abdominal slice varied from 0.5 to 5 mm (mean 2.03 mm, median 1.25 mm). Three experienced radiologists with ten years of experience in cardiac imaging reviewed and analyzed all images, and any disagreement was resolved by consensus.

The pre-contrast studies were evaluated for intramural hematoma, other signs of trauma, and displaced intimal calcification. Each post-contrast CT scan was assessed for a variety of imaging features, including Site and extension of AD, propagation of dissection, Identification of TL and FL, CT attenuation of FL and TL within 3 Cm from intimal tear, Vessels, and branches involved in the dissection, branches arise from TL, FL or both, Flap evaluated in axial cross-section for Mobility; Calcification; Straight or curved; Single line type or multiple line type. False lumen was assessed for the number of FL, calcification on the FL side, calcification in the outer wall of the FL, and FL patency/thrombus, Periaortic fat infiltration. The relative location of TL and FL in the aortic arch and descending aorta. Detection of Intimal tears Number; site of entry tear re-entry tear exit tear. Types of AD Communicating / non-communicating, Type I with large FL/Type II with large TL according to luminal area. Complications include pericardial effusion/hematoma and pleural effusion/hematoma. Size of the following features: Maximum aortic diameter, Maximum flap thickness, FL maximum diameter, Size ratio of the FL to true lumen

***Analysis by virtual CT*:** Entry tears shape type, Intimal flap shape, the display quality of intimal tears, Relation of great branches to flap, Extension of flap into great branches. For every patient, CTVA reconstruction was performed. In order to obtain an accurate lesion localization and description with respect to the major aortic valve and branches, we manually modified the VR thresholds for navigation mode, and spatial rendering produced endoluminal views. All patients received full fly-through navigation with three-dimensional aortic wall reconstruction.

Statistical Analysis:

Microsoft Excel 2007 (Microsoft Corporation, NY, USA) and SPSS (Chicago, IL, USA) version 17 for Microsoft Windows were used for data analysis. The mean, standard deviation, and range were used to present quantitative data, whereas the number and percentage were used to present qualitative data.

RESULTS

This study included 18 patients who were suspected to have acute aortic syndrome and were proved on examination by CT as AD. Their ages ranged from 32 to 86 years, with the mean age being 60.39 years, with male predominance; the ratio of female to male patients was 1:3.

The patients were classified according to the lesion anatomic location as proximal (involving the aortic root or ascending aorta) or distal (below the left subclavian artery). The Debakey and Stanford classification systems were used; in our study, most of the cases were Stanford type A, the least cases were Stanford type B, and according to Debakey classification, most of the cases were type I. They were further classified according to the luminal area and presence of communication into two types of each; in our study, most of the cases were type I with a large false lumen (FL) and communicating.

The intimal tear detected by conventional CT was differentiated into entry tear (ET) and re-entry tear (exit tear); in our study, there were 35 intimal tears, 19 entry tears, and 16 exit tears (Table 1).

The site of entry tears and exit tears were assessed; 10 cases of entry involved the ascending aorta, one in the isthmic portion, and three in the descending thoracic aorta. The exit tear involved the descending thoracic aorta in two cases and the descending abdominal aorta in five cases. The flap was characterized by axial cross-section for mobility, shape, and type; 10 cases were immobile, and eight cases were mobile. Regarding the flap types, seven cases were mostly straight, 11 cases were mostly curved, 15 cases were single line type, and three cases were multiple line type (Table 2).

Thrombosis of FL is detected in 33.3% of cases. Calcification of the flap on the FL side and the outer wall of the FL appear with chronicity of dissection; in our study, six cases had FL thrombosis, 12 cases had no thrombosis, 11 cases had calcified FL outer wall, and seven cases had no calcification. While 10 cases had calcified the FL side of the flap, eight cases had no calcification. The relative location of the true lumen (TL) and FL in the aortic arch and the descending aorta is presented in (Table 3).

Hence, endovascular repair is frequently performed in the true lumen; the VIE pictures of the torn inlet and outlet, in addition to that of the nearby intimal flap, were generated in the true lumen in the majority of cases using the workstation. An appropriate threshold was gradually adjusted during VIE imaging to produce good views that could more clearly reveal the intimal flaps and entry tears with fewer artifacts. Virtual CT provides a unique picture of the aorta from the inside and provides a more accurate specification of tears and flaps; nine cases had irregular entry tears, six cases had rounded ET, two had slit ET, one case had two entry tears with different shape one was slit, and the other was irregular, the intimal flap was irregular in two cases, sheet-like in 10 cases, wave-like in four cases and tubular in two cases, intimal tear display quality was available in three cases, satisfactory in five cases and optimal in 10 cases (Table 4).Also, virtual CT allowed us to detect dissection of small branches as coronary arteries; among 13 cases of type A aortic aneurysm, two cases proved to have dissected coronary arteries by virtual CT that could not be detected by conventional CT (Table 4). Associated complications are listed in (Table 5). By using conventional CT, we can characterize the entry tear according to the site and number; using virtual CTA allowed us to detect the type of entry tear (round, irregular, and slit). Also, regarding the flap by conventional CT, it is divided into two types, single line, and multiple line type, and is seen in axial cross-section; by using virtual CT, there were four types (irregular, sheet-like, wave, and tubular). Additionally, the true spatial connection between the intimal involvement of the tear and nearby structures, such as aneurysms, transmural ulcerations, and other tiny torn flaps, can be more clearly visualized using virtual CT (Fig. 1 &2). The dissection starts at the intimal tear and then propagates either proximally (retrograde), distally (antegrade), bidirectional, and rarely not propagates (Supplementary Fig.1), demonstrating the type of propagation and the extent of dissection in our study.

Table (1): Stanford, Debakey, communication, and luminal area classification and number of intimal and exit tears.

	Number	Percent
Stanford classification		
A	13	72.2%
B	27.8	27.8%
Debakey classification		
I	11	61.1%
II	2	11.1%
IIIa	3	16.7%
IIIb	2	11.1%
Classification according to luminal area		
Type I	13	72.2%
Type II	5	27.8%
Classification according to communication		
Communicating	12	66.7%
Non-communicating	6	33.3%
Number of intimal tears		
Not seen	2	11.1 %
1	13	72.2 %
2	3	16.7 %
Number of exit tear		
Zero	6	33.3 %
1	9	50.0 %
2	2	11.1 %
3	1	5.6 %

Table (2): site of entry tears and exit tears and characterization of edges of tears and dissecting flap characterization.

	Number	Percentage
Site of intimal tear		
Not seen	2	11.1 %
Ascending aorta	10	55.5 %
Immediately distal to the arch	1	5.6 %
Descending thoracic aorta	3	16.6 %
Aortic root and descending thoracic aorta	1	5.6 %
Ascending aorta and descending thoracic aorta	1	5.6 %
Site of exit tear		
Not seen	6	33.3 %
Isthmus	1	5.6 %
Ascending aorta	1	5.6 %
Descending thoracic aorta	2	11.1 %
Descending abdominal aorta	5	27.6 %
Right common iliac	1	5.6 %
Left common iliac	1	5.6 %
Descending abdominal aorta and right common iliac	1	5.6 %

characterization the dissecting flap characterization.

	Number	Percent
Flap type near the intimal tear		
Single line	15	83.3 %
Multiple lines	3	16.7 %
Flap shape in axial cross section		
Straight	7	38.9 %
Curved	11	61.1 %
Flap mobility		
Absent	10	55.6 %
Present	8	44.4 %

Table (3): characterization of FL and relative location of TL to aorta

	Number	Percentage
Calcification on false lumen side of the flap		
Present	10	55.6 %
Absent	8	44.4 %
Calcification on false lumen outer wall		
Present	11	61.1 %
Absent	7	38.9 %
False lumen thrombus		
Present	6	33.3 %
Absent	12	66.7 %
Relative location of true lumen in aortic arch		
Not involved	7	38.9 %
In inner curvature of aortic arch	8	44.4 %
In outer curvature of aortic arch	3	16.7 %
Relative location of true lumen In descending aorta		
Not involved	3	16.6 %
Anterior and to the left of false lumen	5	27.7 %
Anterior and to the right of false lumen	2	11.1 %
To the left of false lumen	4	22.2 %
Posterior and to the right of false lumen	1	5.6 %
Posterior and to the left of false lumen	1	5.6 %
To the left then posterior and to the left of false lumen	1	5.6 %
Anterior then to the right then posterior to false lumen	1	5.6 %

Table (4): Virtual CT appearance, and add value of virtual CTA.

Entry tear shape		
Irregular	Number	9
	Percent	50.0 %
Round	Number	6
	Percent	33.3 %
Slit	Number	2
	Percent	11.1 %
One slit and one irregular	Number	1
	Percent	5.6 %
Total	Number	18
	Percent	100 %
Intimal flap shape		
Irregular	Number	2
	Percent	11.1 %
Sheet like	Number	10
	Percent	55.6 %
Wave like	Number	4
	Percent	22.2 %
Tubular	Number	2
	Percent	11.1 %
Total	Number	18
	Percent	
Intimal tear display quality		
Available	Number	3
	Percent	16.7 %
Satisfactory	Number	5
	Percent	27.7 %
Optimal	Number	10
	Percent	55.6 %
Total	Number	18
	Percent	100 %
Add value of virtual CTA.		
Parameters	Conventional CT	Virtual CT
Classification of entry tear shape	0.0 % classified	5.6 % Slit and Irregular 11.1 % Slit 33.3 % Rounded 50.0 % Irregular
Classification of intimal flap shape	83.3 % Single line 16.7 % Multiple lines	11.1 % Irregular 11.1 % Tubular 22.2 % Wave like 55.6 % Sheet like
Detection of coronary dissection in Stanford type A (13 cases)	0.0 % detected positive	15.4 % detected positive

Table (5): Associated complications

	Absent		Present		Total	
	Number	**Percent**	**Number**	**Percent**	**Number**	**Percent**
Pericardial effusion	11	61.1 %	7	38.9 %	18	100 %
Pericardial hematoma	14	77.8 %	4	22.2 %	18	100 %
Pleural effusion	15	83.3 %	3	16.7 %	18	100 %
Pleural hematoma	15	83.3 %	3	16.7 %	18	100 %

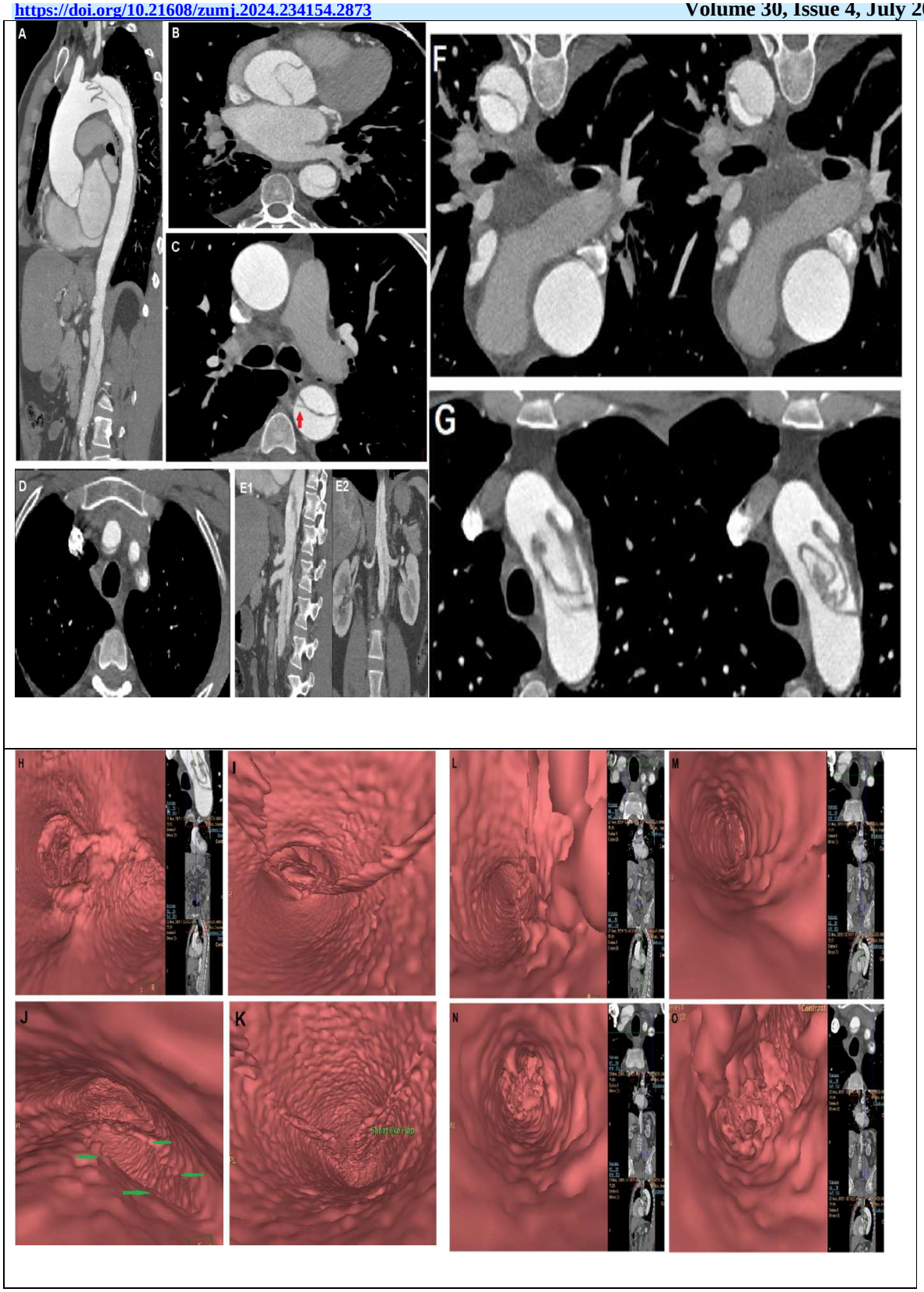

Fig. 1. 70-year-old male patient with acute chest pain showed Stanford Type I A dissection. (A) Contrast enhanced CT sagittal MPR shows dissecting flap involving the aortic root, the sinus of Valsalva and coronary arteries, no intimal flap at the tubular portion and sinu-tubular junction with

aneurysmal dilatation, an intimal dissecting flap involving the arch of the aorta, descending thoracic and abdominal aorta and RT CIA. The TL lies in the inner curvature of the aortic arch, in the descending aorta the TL anterior and to the left of FL. (B &C) Contrast enhanced CT axial MPR show dissecting flap involving the aortic root, the sinus of Valsalva and, no intimal flap at the tubular portion and sinu-tubular junction with aneurysmal dilatation. The dissection extended thoracoabdominal; antegrade in ascending aorta and bidirectional in the descending aorta, the entry tears in the descending thoracic aorta and the exit tear in the descending abdominal aorta.(D) Contrast enhanced CT axial MPR shows dissected supra-aortic branches.

The intimal flaps in axial cross section mostly curved and of single line type seen in (Band C) contrast enhanced CT axial MPR. (E1 and E2) contrast enhanced CT sagittal and axial MPR respectively show celiac artery, SMA, IMA, RT renal artery, one LT renal artery, LCCA arise from TL, the other LT renal artery arises from FL. (F and G) contrast enhanced CT axial MPR cutting dissected descending aorta and aortic arch shows flap mobility. There is no calcification on FL side of the flap but there is cal. in outer wall of FL and there is no thrombus on FL. There is no pericardial effusion, no pleural effusion and the periaortic fat of soft tissue density. By virtual CT, (I and J: virtual CT) shows rounded entry tears. (H: virtual CT at aortic arch) shows dissection flap in the arch, irregular mucosa. (K: virtual CT at descending aorta) shows the flap is sheet like, display quality is grade I of optimal visualization. (L, M, N and O: virtual CT at aortic arch branches) show dissection of the supra-aortic branches, irregularity and roughness of their mucosa.

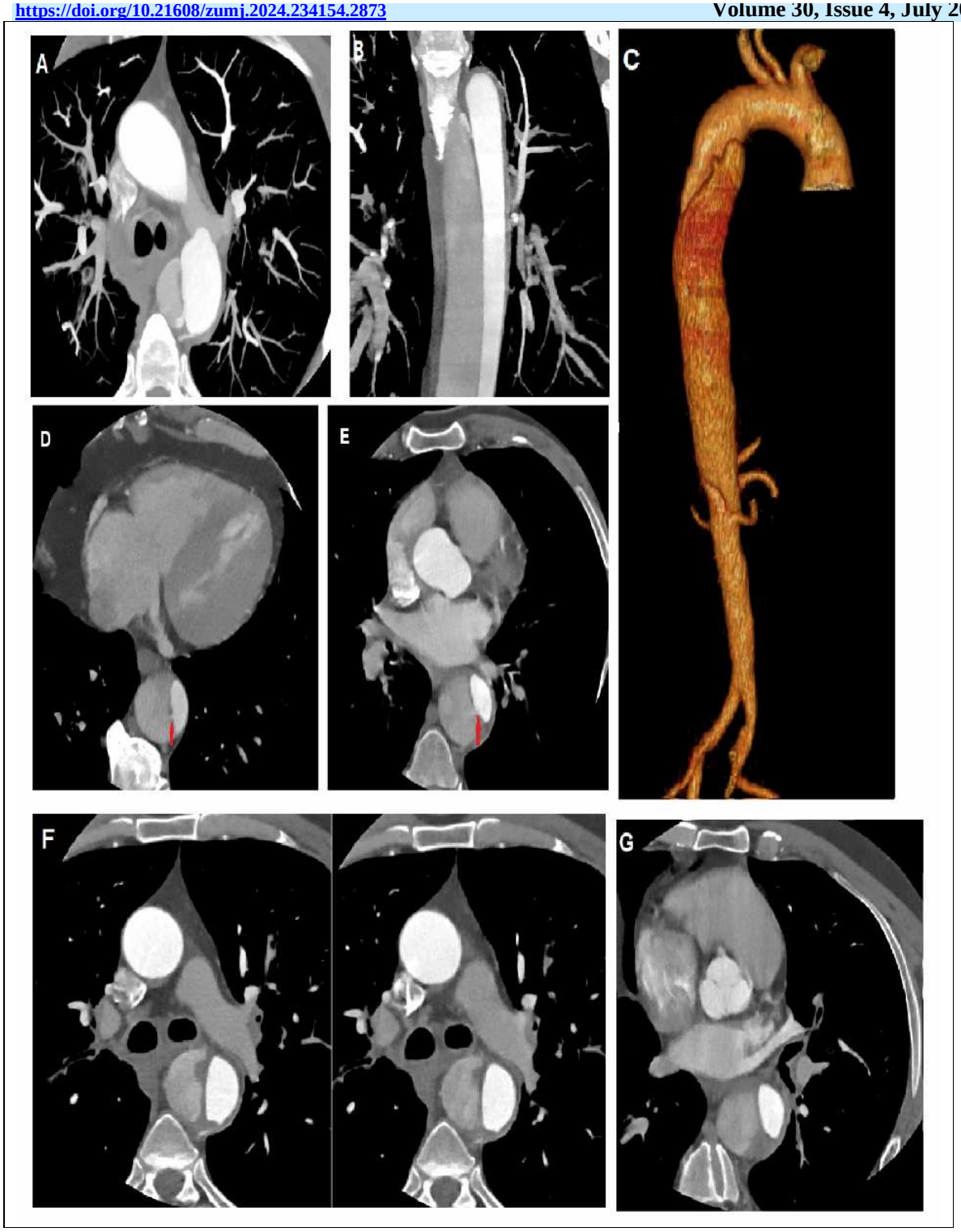
A
B
C
D
E
F
G

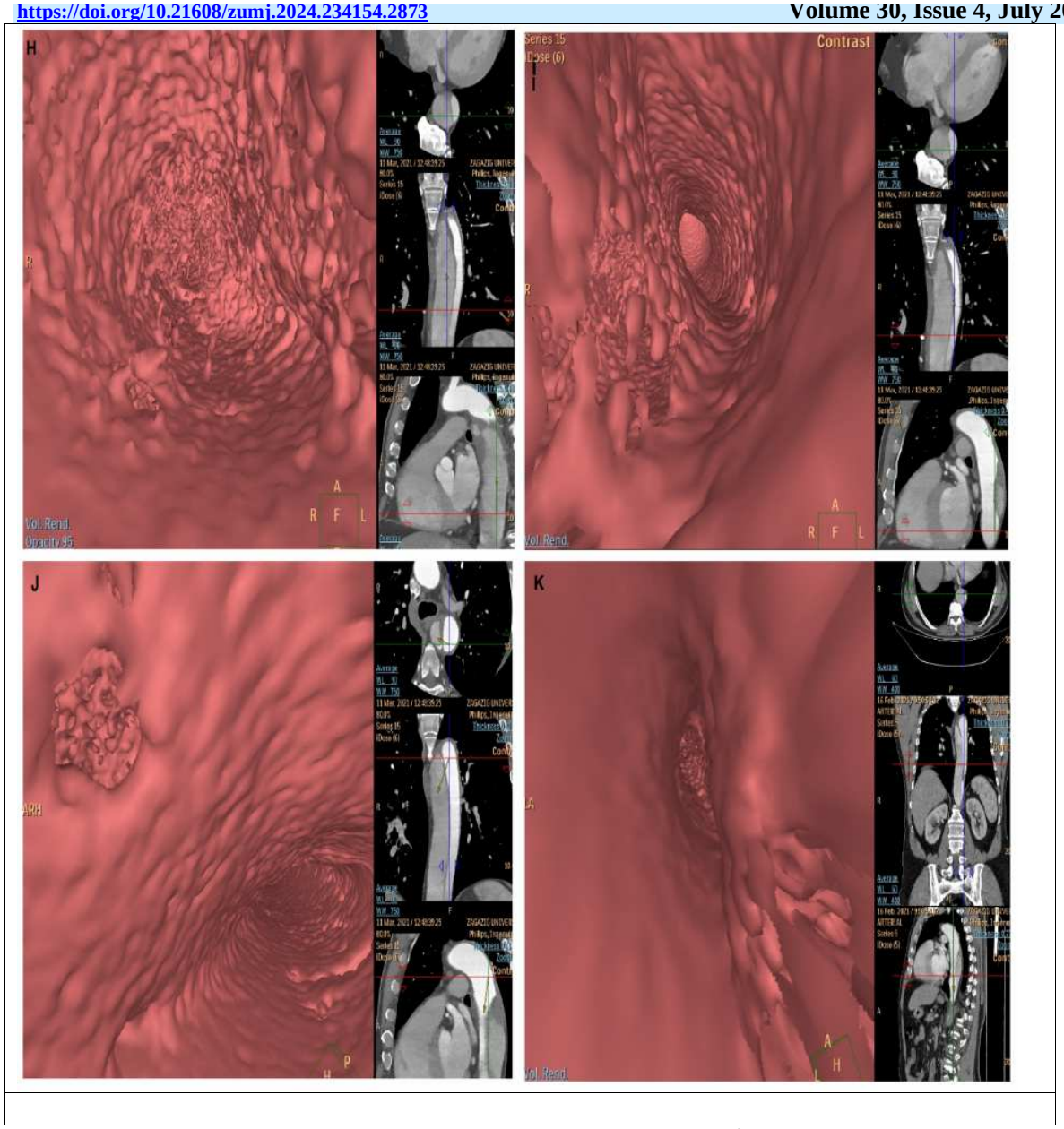

Fig. 2. 54-year-old male patient with acute back pain showed Stanford Type III B dissection. (A and B) Contrast enhanced CT axial and coronal MPR respectively, (C) volume rendering CT showing an intimal flap involving the aorta, extending from just distal to the aortic arch to the abdominal aorta proximal to the level of the renal arteries. (A and B) Contrast enhanced CT axial and coronal MPR respectively show the entry tear in descending thoracic aorta, The dissection extended thoracoabdominal and of bidirectional (antegrade and retrograde) propagation. (D and E) Contrast enhanced CT axial MPR show the two exit tears in the descending thoracic aorta. All the aortic branches not dissected. All arise from TL. (F) Contrast enhanced CT axial MPR shows the intimal flaps in axial cross section which mostly straight and of single line type and there is flap mobility. (G) Contrast enhanced CT axial MPR show thrombus on FL, there is no calcification on FL side of the flap but there is cal. in outer wall of FL. There is no pericardial effusion, no pleural effusion and no periaortic fat infiltration. By virtual CT, (H: virtual CT at FL in descending aorta) shows irregular rough mucosa of FL. (I: virtual CT at TL in descending aorta) shows regular smooth mucosa of TL, the flap is sheet like. (J: virtual CT at ET site) shows rounded entry tear and sheet like dissecting flap. (K: virtual CT) shows compressed small slit shape TL with regular smooth mucosa.

DISCUSSION

This study aimed to assess the role of MDCT in the diagnosis of AD and the added value of virtual CT. 18 patients suspected to have aortic syndrome proved in examination by CT as aortic dissection were included in this study, their ages ranged from 32 to 86 years the mean ages 60.39 ±13.980 years with male predominance (77.8 %) this nearly agree with IRAAD.

IRAD reported that the mean age of presentation in Aortic Dissections is 63 years, and 65% of cases were males. Women were rarely affected, but because of delayed diagnosis and atypical symptoms, they had worse outcomes [7].

Also, Lu et al. [9] compared MSCTA and digital subtraction angiography (DSA) to diagnose AD in 49 non-consecutive cases. Seven cases were females, while 42 were male, with a mean age of 49.6 years.

In agreement was a study by Zhao et al. [6], who discussed the diagnostic value of MSCTA in AAS.

This study nearly agrees; 72.2% of cases were Stanford type A, 27.8% of cases were Stanford type B, and according to Debakey classification, 61.1% of cases were type I, 11.1%cases type II, 16.7%type IIIa, 11.1% were type IIIb.

Chiu et al. [10] noted that the false lumen is typically bigger in caliber than the actual lumen in AAD conditions. This is most likely caused by persistent compression brought on by the false lumen's systolic pressure exceeding that of the true lumen.

For more characterization of dissection, it classified according to the luminal area and communication into two types of each; in our study, 72.2% cases were type I with large false lumen, 27.8% cases were type II with large true lumen, 66.7% cases were communicating and 33.3% cases non communicating type, according to Qi et al. [11] study, the dissection was of large FL in 55.4%. It was of large TL in 44.6%.

About 65% of cases experience intimal tears in the ascending aorta, 10% in the transverse aortic arch, 20% in the proximal descending aorta, and 5% more distally [12].

In this study, intimal entry tears occur in ascending aorta in (55.5 %), the isthmus in (5.6 %), in the proximal descending aorta in (16.6 %), in the aortic root in (5.6 %), in ascending aorta and descending thoracic in the same patient in (5.6 %) and can't detect entry tear due to complete thrombosis in (11.1 %).

Lu et al. [9] reported that Initial entry tears were visible in 95.92% of the cases, and they were absent in just two of the DeBakey type I instances. In 87.76% of the sample, there was only one first-entry tear, whereas in four cases, there were two initial-entry tears (8.16%). Thirty-one people, or 77.55%, had less than two re-entries. The aortic segment was frequently the site of re-entrance. In 78.7% of cases, the false lumen diameter was bigger than the diameter of the genuine lumen. In addition, 10% of patients had a true lumen with a diameter of less than 1.0 cm. The true lumen compression of the aorta by the false lumen was frequently seen in cases (48.65%).

Nagra et al. [13] noted that MPR, curved planner, and VR all exhibited a display rate of 100% for true and false lumens; however, MIP only offered a display rate of 67.35%. The display of input site number and position differed substantially between MSCTA and DSA when put side by side ($P< 0.05$).

Exit tears in this study occur in the ascending aorta in (5.6%), in the isthmus in (5.6%), in descending thoracic aorta in (11.1%), in descending abdominal aorta in (27.6%), in the iliac artery in (11.2%), in descending abdominal aorta and RT iliac artery in the same case in (5.6%), and not seen in (33.3%), while in Qi et al. [12] study exit tear occur in ascending aorta in 6.98%, in aortic arch in 20.9%, in descending thoracic in 4.56%, in descending abdominal in 39.5%, in iliac artery in 27.9%.

In this study, the intimal flap near the entry tear was of single line type (83.3%) and multiple line type (16.7%); this doesn't agree with the study by Qi et al. [11], where the flap

was of single line type in 34.8% and multiple line type in 65.2%, this can be explained by selection bias between the two studies.

Regarding the type of propagation in this study was antegrade in (27.8%), bidirectional in (50%), no propagation in (11.1%), and can't assessed in (11.1%) due to complete thrombosis of FL in (11.1%); this disagrees with Qi et al. [11] study that had antegrade propagation in 40.2%, retrograde propagation in 46.7% and bidirectional propagation in 13.1%, this can be explained by selection bias between the two studies.

Inadequate outflow or an imbalance between inflow and outflow increases pressure in the false lumen, leading to false lumen enlargement and aneurysm formation over time or acute true lumen compression. The extent of AD shows more extensive pre-existing aortic disease. The more the false lumen is drained by big unobstructed branches originating from the false lumen, the lower the chance of complications [14].

In this study, the dissection extension was thoracic in three cases (16.7%) and thoracoabdominal in 15 cases (83.3%) with Sailer et al. [14] where 11 cases (13%) were thoracic, and 72 cases (87%) were of thoracoabdominal extension as his study works on type B only. Our study works on both types A and B for better assessment of dissection and late squeals; each aortic branch supply was defined.

Sherk et al. [12] stated that in so-called distal AD, the real and false lumens typically lie in the following positions: He stated that the distal FL is found in the left side of the aorta, where it terminates in the left iliac artery, in 80% of cases, and in the right side of the aorta, where it terminates in the right iliac artery, in 10% of cases. 10% of the cases showed variable termination.

In this study, the distal FL is located on the right side of the aorta in (61.1 %), the distal FL is located on the left side in (16.7 %), FL encircles TL in (5.6 %) and not involved in (16.6 %); this difference in the ratio in our study may be due to a smaller number of patients in our study.

In this study, FL thrombosis was detected in (33.3%) of cases and absent in (66.7%) of cases; this agrees with a study by Sailer et al. [14], where thrombosis of FL was detected in 47% of cases and absent in 53% of cases. In contrast, in Sailer et al. [14] study, 93% had a moving flap; in our study, only (44.4%) had a moving flap, and (55.6%) had no moving flap.

Lu et al. [9] observed that, regarding the assessment of true and false lumens in comparison. Before surgery, it is crucial to identify specific details, such as thrombosis, the size ratio of the TL to FL, and whether the critical vascular branches are supplied with blood by the true lumen.

The TL was larger than FL at the middle ascending aorta in three cases and smaller in five cases; in 10 cases, MAA was not involved by dissection; the TL was larger than FL at the isthmus in four cases, smaller in six cases, equal in one case and not involved in seven cases; the TL was larger than FL at midway between left subclavian and celiac artery in four cases, smaller in 11 cases and not involved in three cases; the TL was larger than TL in four cases, smaller in 11 cases and not involved in three cases.

According to Sailer et al. [14], 95% of his study cases had TL in the inner curvature of the arch of the aorta, and 5% of cases had TL in the outer curvature.

This study doesn't agree with him. In this study (72.7%) had TL in the inner curvature, (27.2%) had TL in the outer curvature, and (38.9%) had the arch not involved.

Aortic dissection may be associated with some complications, as periaortic fat infiltration in 72.1%, pericardial effusion in 38.9%, haemopericardium in 22.2%, and pleural effusion in 16.7% and pleural hematoma in 16.7%.

Respecting therapeutic and diagnostic purposes, it is crucial to identify the exact position of the entrance tear. Virtual CT allows the development of intraluminal views that highlight the communication between real and false lumens by traversing through the aorta and its branches, including the coronary branches [16].

In virtual CT, the entry tear was rounded in (33.3%), irregular in (50%), slit in (11.1%) and one entry tear and another irregular tear in the same case in (5.6%), the quality of displaying of intimal tear was optimal in (55.5%), satisfactory in (27.7%) and available in (16.7%). This nearly agrees with the results of Qi et al. [11], where the tear was round in 29.5 %, irregular in 60.2%, and slit in 10.2%.

As a consequence, virtual CTA is an important tool for viewing the 3D structures of intimal rips and flaps. This expands our understanding of endovascular anomalies and gives more data for evaluation, management, and follow-up. The torn inlet and outlet were displayed at 95.7% and 90.7%, respectively, with an acceptable presentation of the entry tear (grades 1 and 2 display quality) at 90.9%. Virtual CTA revealed that 61.4% of the flaps were tubular, wavy, or irregular, whereas 60.2% of entry tears were uneven in shape [11].

Qi et al. [11] stated that the entry tear and intimal flap are seen in 3D using virtual CTA, which may overcome some of the drawbacks of conventional CT.

Sun et al. [16] stated that it may be challenging to identify the intimal flap on CT imaging if the false lumen is thrombosed; this makes it challenging to differentiate AAD from mural thrombus or intramural hematoma. Even in the presence of substantially stenosed lumens, intraluminal imaging can overcome the limitations of traditional visualizations.

This study had some limitations. First, it had a relatively small sample size. Secondly, our study was a retrospective study, which could limit the generalizability of our findings to larger populations. Also, the nature of the rare disease was that it took more than two years to recruit a sample size. In addition, the use of multiple scanners with different image quality could affect the results.

CONCLUSIONS

Because of its efficiency, accessibility, and sensitivity, MDCTA is considered the preferred approach for diagnosing individuals with suspected aortic dissection. Aortic dissection should be assessed with VIE in addition to cross-sectional and multiplanar reformatted CT images to detect the exact position of anatomic details, especially the aortic branches concerning their relationship to the dissection, for better characterization of AD flap and tears, By Virtual CT vessel involvement can be confirmed even the tiny artery branches such as coronary arteries.

Conflicts of interest: The authors declare that they have no conflicts of interest.

Funding sources: The authors have no funding to report.

REFERENCES

1. **Liu N, Wu Y, Le K, Mao Q, Zhou M, Yu X, et al**. The Application of Computed Tomography Angiography in Aortic Dissection. World J. Cardiovasc. Dis. 2021;11:464–75.
2. **Evangelista A, Isselbacher EM, Bossone E, Gleason TG, Eusanio MD, Sechtem U, et al**. Insights From the International Registry of Acute Aortic Dissection: A 20-Year Experience of Collaborative Clinical Research. Circulation. 2018;137:1846–60.
3. **Gawinecka J, Schnrath F, Von Eckardstein A**. Acute aortic dissection: pathogenesis, risk factors and diagnosis. Swiss Med Wkly [Internet]. 2017 [cited 2023 Oct 2]; Available from: https://smw.ch/index.php/smw/article/view/2356
4. **Hansen NJ**. Computed Tomographic Angiography of the Abdominal Aorta. Radiologic Clinics of North America. 2016;54:35–54.
5. **Gu G, Wan F, Xue Y, Cheng W, Zheng H, Zhao Y, et al**. Lumican as a novel potential clinical indicator for acute aortic dissection: A comparative study, based on multi-slice computed tomography angiography. Exp Ther Med. 2016;11:923–8.
6. **Zhao D-L, Liu X-D, Zhao C-L, Zhou H-T, Wang G-K, Liang H-W, et al**. Multislice spiral CT angiography for evaluation of acute aortic syndrome. Echocardiography. 2017;34:1495–9.
7. **Nienaber CA, Clough RE, Sakalihasan N, Suzuki T, Gibbs R, Mussa F, et al**. Aortic dissection. Nat Rev Dis Primers. 2016;2:16053.
8. **Nienaber CA, Clough RE**. Management of acute aortic dissection. Lancet. 2015;385:800–11.
9. **Lu D, Li C-L, Lv W-F, Ni M, Deng K-X, Zhou C-Z, et al**. Diagnostic value of multislice computerized tomography angiography for aortic dissection: A comparison with DSA. Exp Ther Med. 2017;13:405–12.
10. **Chiu KWH, Lakshminarayan R, Ettles DF**. Acute aortic syndrome: CT findings. Clin Radiol. 2013;68:741–8.

11. **Qi Y, Ma X, Li G, Ma X, Wang Q, Yu D**. Three-Dimensional Visualization and Imaging of the Entry Tear and Intimal Flap of Aortic Dissection Using CT Virtual Intravascular Endoscopy. PLoS One. 2016;11:e0164750.
12. **Sherk WM, Khaja MS, Williams DM**. Anatomy, Pathology, and Classification of Aortic Dissection. Tech Vasc Interv Radiol. 2021;24:100746.
13. **Nagra K, Coulden R, McMurtry MS**. A type A aortic dissection missed by non-cardiac gated contrast-enhanced computed tomography due to an aortic root dissection flap masquerading as an aortic valve apparatus: a case report. J Med Case Rep. 2013;7:285.
14. **Sailer AM, van Kuijk SMJ, Nelemans PJ, Chin AS, Kino A, Huininga M, et al**. Computed Tomography Imaging Features in Acute Uncomplicated Stanford Type-B Aortic Dissection Predict Late Adverse Events. Circ Cardiovasc Imaging. 2017;10:e005709.
15. **Criado FJ**. Aortic dissection: a 250-year perspective. Tex Heart Inst J. 2011;38:694–700.
16. **Sun Z, Al Moudi M, Cao Y. CT** angiography in the diagnosis of cardiovascular disease: a transformation in cardiovascular CT practice. Quant Imaging Med Surg. 2014;4:376–96.

SUPPLEMENTARY FILES

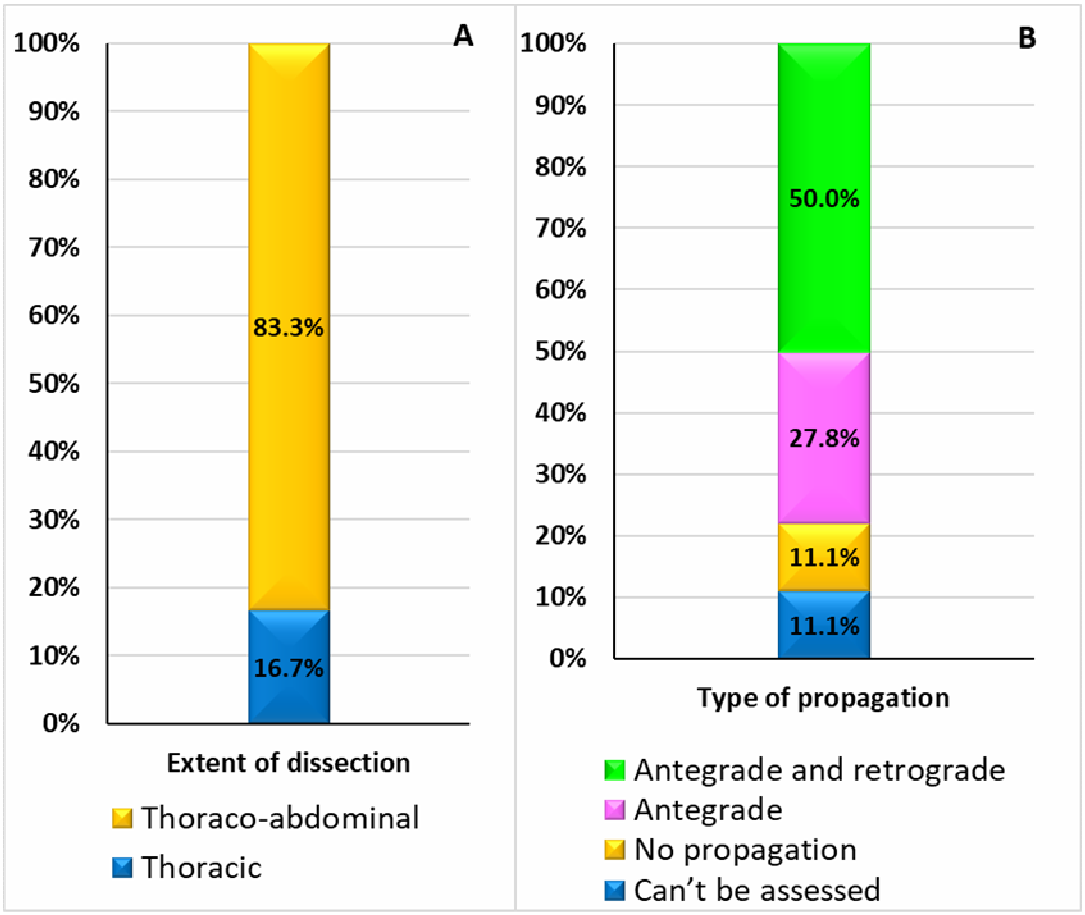

Supplementary Fig. 1. Bar chart showing type and extent of propagation.

Citation: